Drillstring Washout Diagnosis using Friction Estimation and Statistical Change Detection

Anders Willersrud, Mogens Blanke, *SM IEEE,*, Lars Imsland, Alexey Pavlov

***Abstract*—In oil and gas drilling, corrosion or tensile stress can give small holes in the drillstring, which can cause leakage and prevent sufficient flow of drilling fluid. If such *washout* remains undetected and develops, the consequence can be a complete twist-off of the drillstring. Aiming at early washout diagnosis, this paper employs an adaptive observer to estimate friction parameters in the nonlinear process. Non-Gaussian noise is a nuisance in the parameter estimates, and dedicated generalized likelihood tests are developed to make efficient washout detection with the multivariate t-distribution encountered in data. Change detection methods are developed using logged sensor data from a horizontal 1400 m managed pressure drilling test rig. Detection scheme design is conducted using probabilities for false alarm and detection to determine thresholds in hypothesis tests. A multivariate approach is demonstrated to have superior diagnostic properties and is able to diagnose a washout at very low levels. The paper demonstrates the feasibility of fault diagnosis technology in oil and gas drilling.**

***Index Terms*—Managed pressure drilling, fault diagnosis, statistical change detection, adaptive observer, multivariate t-distribution, generalized likelihood ratio test**

I. Introduction

Drilling is a major part of the total oil or gas field development cost. As the easy available reservoirs are being depleted, there is a trend that boundaries for drilling is pushed in the sense of more extreme environments, such as the arctic, or deep wells with high pressure and high temperature. With increasing depth and drilling at more remote locations, the cost of drilling is further increased and it is essential to minimize non-productive time, that amounts to 20-25 % of total time in operation [1].

Different incidents can happen downhole or topside that cause downtime, or even abandonment of a well. Emerging advanced drilling methods such as *managed pressure drilling* (MPD) [1], [2] brings along new instrumentation to the rig, which allows one to have methods for detecting abnormal situations. One such situation is *drillstring washout*, which will be studied in this paper. A drillstring washout is a hole or cracks in the drillstring caused by wear, such as corrosion or tensile stress [3]. Such weakness can result in a complete twist-off of the pipe, which may cause an extra three to twelve days of drilling, in worst case abandonment of the well [4]. Early yet sure diagnosis of a drillstring washout is essential. The challenge is that a small washout gives tiny changes in pressure and flow rate of the circulated drilling fluid, and is difficult to detect in noisy measurements signals. In addition to detecting the occurrence of the washout it is of great value to isolate the position of the defect, making inspection and replacement more effective.

Detection of other critical incidents have been studied using different detection methods. Probably the most studied case is an influx of formation fluid, or *kick*, see [5], [6], [7], [8]. Others are *lost circulation* of drilling fluid to the formation, *pack-off* of drilling cuttings around the drillstring, and *plugging* of the drill bit nozzles. All of these will affect drilling operation. Simulation and detection of different downhole drilling incidents, including drillstring washout, were discussed in [9] with some tests on real data in [7]. There a high fidelity model was fitted to data and used to detect abnormalities. Knowledge-modeling was used for classification of different incidents by [10] and a Bayesian network was shown to detect sensor and process faults in [11].

A challenge with monitoring and diagnosis of downhole conditions in drilling is the lack of measurements. Most commonly, low frequency measurements with mud pulse telemetry from the downhole assembly has been available [1]. With high data rate, low latency transmission from downhole sensors, actions can be taken at an earlier stage in order to avoid borehole stability problems [12]. Recently, *wired drill pipe technology* has emerged as a technology with distributed sensors along the drillstring, providing measurements at high sample rate in real time [1], [13].

Although increased instrumentation facilitates increased diagnosis, there are still problems with measurement noise. Different statistical methods can be applied in order to increase detection. In [5], a statistical cumulative sum (CUSUM) algorithm was applied in order to increase kick detection while maintaining a low false alarm rate. In [14], skewness of the statistical distribution was used to detect poor hole cleaning. An adaptive observer for friction estimation was presented in [15] and applied on data in [16], but direct washout diagnosis was not feasible due to very poor signal to noise properties on the parameter estimates.

This paper proposes to use statistical change detection methods to diagnose downhole drilling incidents. The focus

Manuscript submitted February 28, 2014 to IEEE Transactions on Control Systems Technology.

This work was supported by Statoil ASA and the Norwegian Research Council (NFR project 210432/E30 Intelligent Drilling).

A. Willersrud (corresponding author) and L. Imsland are with the Department of Engineering Cybernetics, Norwegian University of Science and Technology, N-7491 Trondheim, Norway, anders.willersrud, lars.imsland@itk.ntnu.no.

M. Blanke is with the Automation and Control Group, Department of Electrical Engineering, Technical University of Denmark, DK-2800 Kgs. Lyngby, Denmark and is affiliated with the AMOS Centre of Excellence, Department of Engineering Cybernetics at NTNU in Trondheim, mb@elektro.dtu.dk.

A. Pavlov is with the Department of Advanced Wells and Enhanced Oil Recovery, Statoil Research, N-3905 Porsgrunn, Norway, alepav@statoil.com.

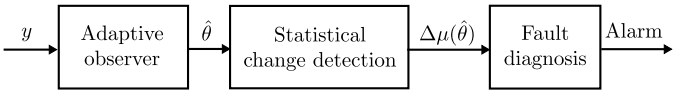

Figure 1. Overview of fault diagnosis method using an adaptive observer and statistical change detection for fault diagnosis, where y are measurements, $\hat{\theta}$ are estimated parameters, and $\Delta\mu(\hat{\theta})$ is the change in mean of the estimated parameters.

is on drillstring washout. The proposed method, depicted in Fig. 1, consists of using a reasonably simple mathematical model together with a nonlinear adaptive observer to estimate a set of friction parameters and combine this with dedicated change detection. The estimated parameters will remain (close to) constant during normal operation, but change when there is a washout in the system. Data from a medium scale flow loop designed and tested by the oil and gas company Statoil ASA is used to test the diagnosis method. Due to noise in the measurements the friction estimates are shown to be noticeably affected. Detection and isolation possibilities are studied using the changes that develop in estimated parameters during a washout. Dedicated change detection algorithms are derived for the multivariate t-distribution that is observed from data, based on a generalized likelihood ratio test (GLRT) approach. A GLRT for each parameter is tested against a threshold using univariate probability distributions of the noise, and changes to all parameters jointly can be considered using multivariate distributions. Detectors are derived for both univariate and multivariate distributions and their performances are compared.

Referring to Fig. 1, the scope of the paper is as follows. Sec. II presents the test rig and test scenarios, Sec. III presents the nonlinear dynamic model of the process, and the nonlinear adaptive observer used for parameter estimation (first block in the figure). Sec. IV motivates the need for statistical change detection, and Sec. V presents an analysis of the noise distribution of the estimated parameters. A dedicated diagnosis scheme is derived in Sec. VI for the multivariate t-distribution at hand (second block), and isolation of the washout position is analyzed in Sec. VII (third block). Findings are validated using experimental data in Sec. VIII. A discussion and conclusion completes the paper.

II. Flow-loop test facility

To test the diagnosis methodology, we will use data from tests on managed pressure drilling technology conducted by Statoil in a 1400 m horizontal flow loop test setup at premises of the International Research Institute of Stavanger (IRIS), Norway. The flow loop was rigged with the possibility of emulating various faults including drillstring washout.

Fig. 2 shows a schematics with drillstring washout highlighted, and parts of the physical setup is shown in Fig. 3. Water is used as drilling fluid and pumped by a piston rig pump with flow rates in the range of 0–2000 L/min (0–0.033 m^3/s). The drill bit consists of three parallel valves, and the pipes are 700 meter circular steel pipes of 0.124 m and 0.155 m inner diameter, for drillstring and annulus respectively. The flow loop is instrumented with topside measurements including

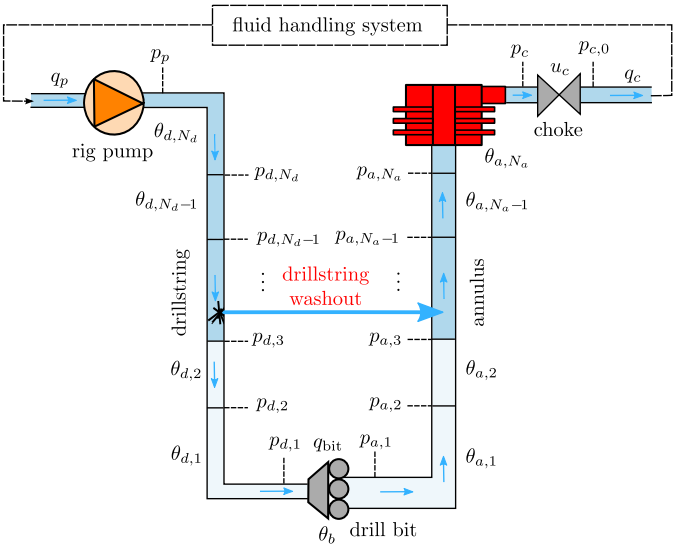

Figure 2. Drilling system with measurements p, q, choke opening u_c, and friction parameters θ. A drillstring washout is a leakage from the drillstring to the annulus, resulting in less flow in the lower part of the system and drill bit.

standpipe and choke pressure, and pump and choke flow. Four pressure sensors in the annulus and one in the drillstring, upstream the bit, emulate a wired drill pipe. The technology quality for wired drill pipe pressure sensors is presently not as good as the pressure sensors used in the flow loop. Whether the accuracy is sufficient for the use we propose here, has not been investigated.

Figure 3. Flow-loop setup components for drillstring washout and gas injection (left) and for drill bit nozzles (right).

Although the flow loop is designed to capture key dynamics in a real drilling circulation system, there are some obvious differences. Since the loop is horizontal, the effects of gas expanding as is percolates up the annulus will not be captured. Other differences is lack of annular effects and drillstring rotation. Cuttings (crushed formation rocks) transportation is also not included. However, the flow loop uses pumps and chokes that are used in real drilling, and measurements will be affected by bias and noise as at a real rig.

Data from a series of tests carried out by Statoil at the test rig is used to test the fault diagnosis method. Even though several incidents are tested, for clarity of presentation only the drillstring washout case will be used in this paper. Diagnosis

of other incidents is the topic in [17]. Drillstring washout is a challenging case with small changes to pressure due to friction, without any net change of flow in and out of the well. To emulate drillstring washout, a valve located half way along the flow loop was gradually open, releasing the flow from the drillstring section of the flow loop to the annulus section.

Table I
FLOW-LOOP PHYSICAL PARAMETERS.

$\beta_{d,a}$	2.2×10^9 Pa	Effective bulk modulus
$\rho_{d,a}$	$1000\,\mathrm{kg/m^3}$	Drilling fluid density
M_a	3.74×10^7 Pa s^2/m^3	Integrated density per cross section
M_d	5.81×10^7 Pa s^2/m^3	Integrated density per cross section
V_a	$13.2\,\mathrm{m^3}$	Volume of fluid in annulus
V_d	$8.56\,\mathrm{m^3}$	Volume of fluid in drillstring
h_{TVD}	$2.14\,\mathrm{m}$	True vertical depth of bit
L_d, L_a	$700\,\mathrm{m}$	Length of drillstring/annulus

III. SYSTEM MODEL AND ADAPTIVE OBSERVER

The model-based fault diagnosis method in this paper is based on parameter estimation using the simplified hydraulics model in [18] as a process model together with an adaptive observer. As the authors argue, the simple model manages to capture the key components of the flow dynamics in drilling. Furthermore, a high-fidelity model with many parameters may not give a better result in practice, due to challenges in configuration and calibration. However, the simple model has some limitations. In realistic situations, the particular *bottom hole assembly* (tools at the end of the drillstring) used may give other setups near the bottom which may imply that detected changes in friction can be caused by other incidents than those considered herein. Moreover, we assume that the friction pressure loss is in steady state, which means that care must be taken in interpreting detections in periods just after known transients such as changing pump rates, drilling bit off bottom, and change of drillstring rotational velocity.

The simple model has been applied for estimation and control purposes in [8], [19], [20], [21]. This section presents the model as well as the adaptive observer utilizing wired drill pipe measurements. The adaptive observer was derived in [15], and used in a preliminary study on fault diagnosis of the flow loop data in [16], with simpler assumptions about the noise probability distribution, detecting changes to each friction parameter separately.

A. Simplified hydraulic model

Referring to Fig. 2, let p_p be the pressure at the pump, p_c be the pressure upstream the choke, and q_{bit} the flow through the bit. The pump flow is denoted by q_{p}, and q_c is flow through the choke. The model used is based on the model in [18], given by

$$\frac{dp_p}{dt} = \frac{\beta_d}{V_d}(q_p - q_{\mathrm{bit}}), \tag{1a}$$

$$\frac{dp_c}{dt} = \frac{\beta_a}{V_a}\left(q_{\mathrm{bit}} - q_c(p_c, u)\right), \tag{1b}$$

$$\frac{dq_{\mathrm{bit}}}{dt} = \frac{1}{M}\left(p_p - p_c - F(\theta, q_{\mathrm{bit}}) - (\rho_a - \rho_d)gh_{\mathrm{TVD}}\right), \tag{1c}$$

where ρ_j is the density, V_j the volume, and β_j the bulk modulus of the control volume indexed $j \in \{d, a\}$ for drillstring and annulus, respectively. The true vertical depth of the well is h_{TVD}, g is the acceleration of gravity, and the integrated fluid density per cross section is $M = \int_0^L \frac{\rho(x)}{A(x)}dx$ where L is the total length from pump to choke, and $A(x)$ is the cross section at position x. The unknown friction parameter vector θ is estimated by the adaptive observer. The total friction is modeled by

$$F(\theta, q) = \theta_b f_b(q) + \sum_{i=1}^{N_d} \theta_{d,i} f_d(q) + \sum_{i=1}^{N_a} \theta_{a,i} f_a(q), \tag{2}$$

where $f_d(q)$, $f_b(q)$, and $f_d(q)$ model the flow characteristics in the drillstring, bit, and annulus, respectively, and θ is a vector of assumed constant friction parameters to be estimated. The friction is more accurately modeled by complex models depending on well geometry and the non-Newtonian properties of drilling fluids, but in the spirit of simple models to be updated by measurements, we will here assume that $f(q)$ is given by $f(q) = q$ for laminar flow and $f(q) = q^2$ for turbulent flow. The flow through the choke is given by

$$q_c(p_c, u) = \mathrm{sgn}(p_c - p_{c,0}) g_c(u_c) \sqrt{|p_c - p_{c,0}|}, \tag{3}$$

where $g_c(u_c)$ is the choke characteristics found empirically for choke opening $u_c \in [0, 100]$, $p_{c,0}$ is the pressure downstream the choke.

Wired drill pipe technology extends the number of pressure measurements downhole. Let $p_{d,i}, i \in \{1, \ldots, N_d\}$ be the measurements in the drillstring, and $p_{a,i}, i \in \{1, \ldots, N_a\}$ in the annulus, see Fig. 2. The pressure difference is a function of friction and hydrostatic pressure,

$$p_{d,i} = p_{d,i+1} - \theta_{d,i} f_d(q) + G_{d,i}, \tag{4a}$$

$$p_{a,i} = p_{a,i+1} + \theta_{a,i} f_a(q) + G_{a,i}, \tag{4b}$$

where $G_{j,i} = \rho_j g(h_{j,i} - h_{j,i+1})$ is the hydrostatic pressure difference between sensor $p_{j,i}$ at depth $h_{j,i}$ and sensor $p_{j,i+1}$ at depth $h_{j,i+1}$. The corresponding friction between the sensors is given by $\theta_{j,i} f_j(q)$, where $\theta_{j,i}$ is the constant friction parameter and $f_j(q)$ is the flow characteristics in the drillstring and annulus, respectively. For typical flow rates in the test rig the Reynolds number is large enough to indicate turbulent flow in both drillstring and annulus, giving $f_d(q) = f_a(q) = q^2$, which also was found empirically in [17]. The pressure drop over the drill bit is given by

$$p_{a,1} = p_{d,1} - \theta_b f_b(q), \tag{5}$$

where θ_b is the friction parameter in the drill bit. The flow characteristics $f_b(q)$ is typically given by $f_b(q) = q^2$, see, e.g., [22].

B. Nonlinear adaptive observer

Estimation of parameters in the nonlinear system could be achieved by extensions to the extended Kalman filtering (EKF) techniques that estimate noise covariance online and hence would not need knowledge of noise and process disturbance covariances. This is described for linear systems in [23],

and [24] extended the EKF to continuous nonlinear systems with discrete time measurements. Also the later particle filter approaches could be applied. Here, a nonlinear observer approach is used that is based on deterministic stability analysis but still relies on persistent excitation to get parameter convergence.

An adaptive observer for system (1) was suggested in [15] and is repeated here for completeness. The model is developed such that all states are measured, and such that the friction parameters, θ, are unknown but constant (on the time scale considered here) in the fault-free case. The system (1) can be written as

$$\dot{x} = \alpha(x,u) + \beta(x)\theta, \tag{6a}$$
$$z = \eta(x,z) + \lambda(x)\theta, \tag{6b}$$

where $x(t) \in \mathbb{R}^{N_x}$ are the states, $z(t) \in \mathbb{R}^{N_z}$ are the additional measurements, $u(t) \in \mathbb{R}^{N_u}$ are the inputs, $\theta \in \mathbb{R}^{N_\theta}$ are unknown parameters, and $\alpha(x,u) \in \mathbb{R}^{N_x}$, $\beta(x) \in \mathbb{R}^{N_x \times N_\theta}$, $\eta(x,z) \in \mathbb{R}^{N_z}$ and $\lambda(x) \in \mathbb{R}^{N_u \times N_\theta}$ are locally Lipschitz functions. The observer is based on a nonlinear observer in [25], adapted to the system representation (6) with additional measurements z. It is assumed that z in (6b) is given explicitly.

Specifically, the system (1) with measurements (4) written on the form (6) will have system vectors and matrices

$$x = \begin{bmatrix} p_p,\ p_c,\ q_{\text{bit}} \end{bmatrix}^\top,\ u = \begin{bmatrix} q_p,\ u_c \end{bmatrix}^\top, \tag{7a}$$
$$z = \begin{bmatrix} p_{d,1},\ \ldots,\ p_{d,N_d},\ p_{a,1},\ p_{a,1},\ \ldots,\ p_{a,N_a} \end{bmatrix}^\top, \tag{7b}$$
$$\theta = \begin{bmatrix} \theta_{d,1},\ \ldots,\ \theta_{d,N_d},\ \theta_b,\ \theta_{a,1},\ \ldots,\ \theta_{a,N_a} \end{bmatrix}^\top, \tag{7c}$$

$$\alpha(x,u) = \begin{bmatrix} \frac{\beta_d}{V_d}(u_1 - x_3) \\ \frac{\beta_a}{V_a}(x_3 + u_2 - q_c(x_1,u_3)) \\ \frac{1}{M}(x_1 - x_2 - (\rho_a - \rho_d)g h_{\text{TVD}}) \end{bmatrix}, \tag{7d}$$

$$\beta(x) = \begin{bmatrix} 0 & & 0 \\ 0 & \cdots & 0 \\ -\frac{1}{M}x_3^2 & & -\frac{1}{M}x_3^2 \end{bmatrix}, \tag{7e}$$

$$\lambda(x) = \begin{bmatrix} -x_3^2 & & \\ & \ddots & \\ & & x_3^2 \end{bmatrix}, \tag{7f}$$

$$\eta(x,z) = \Big[z_2 + G_{d,1},\ \ldots,\ z_{N_d} + G_{d,N_d-1}, \tag{7g}$$
$$x_1 + G_{d,N_d},\ z_1,\ z_{N_d+3} + G_{a,1},\ \ldots,$$
$$z_{N_d+N_a+1} + G_{a,N_a-1},\ x_2 + G_{a,N_a} \Big]^\top.$$

Theorem 1 (Willersrud and Imsland [15]): Given an observer on the form

$$\dot{\hat{x}} = \alpha(x,u) + \beta(x)\hat{\theta} - K_x(\hat{x} - x), \tag{8a}$$
$$\dot{\hat{\theta}} = -\Gamma\beta^\top(x)(\hat{x} - x) - \Lambda\lambda^\top(x)(\hat{z} - z), \tag{8b}$$
$$\hat{z} = \eta(x,z) + \lambda(x)\hat{\theta}, \tag{8c}$$

where $K_x, \Lambda, \Gamma > 0$ are tuning matrices, and with $\dot{\theta} = 0$. Let $e_x = \hat{x} - x$ and $e_\theta = \hat{\theta} - \theta$ be variables for the error dynamics, where $e = \begin{bmatrix} e_x^\top, & e_\theta^\top \end{bmatrix}^\top = 0$ is an equilibrium point. Then $e = 0$ is globally exponentially stable if

$$\Gamma^{-1}\Lambda\lambda^\top(\cdot)\lambda(\cdot) - \beta^\top(\cdot)K^\top K\beta(\cdot) > kI_{N_\theta}, \tag{9}$$

for some constant $k > 0$, where $K = \frac{1}{2}(I_{N_x} - K_x^{-1})$, and $I_N \in \mathbb{R}^{N \times N}$ is the identity matrix.

The proof of Thm. 1 is given in [15] and is based on a Lyapunov function for the error dynamics (see also, e.g., [25], [26]). Note that if $\beta(\cdot)$ is bounded and $\lambda^\top(\cdot)\lambda(\cdot) > 0$, there exist some tuning parameters K_x, Γ and Λ such that (9) is fulfilled. The matrix function $\beta(\cdot)$ is bounded as the physical flow $x_3 = q_{\text{bit}}$ through the system always will be bounded, while $\lambda^\top(\cdot)\lambda(\cdot) > 0$ can be interpreted as a requirement for persistence of excitation and will be fulfilled whenever there is flow through the well. If $\Gamma > 0$ and $\Lambda > 0$ are fixed, it can be seen from (9) that there is a maximum value of $K^\top K$, thus a minimum and maximum value of K_x, with $K^\top K$ smallest for $K_x = I_{N_x}$. Furthermore, (9) shows that there is a lower bound on $\Gamma^{-1}\Lambda$ as a function of K_x, $\beta(\cdot)$ and $\lambda(\cdot)$, where increasing Λ and Γ gives higher noise magnification, while lowering them gives slower parameter updates. Since these estimates are used for detection, it is desirable with fast updates of estimated parameters after a change, giving requirements on the tuning matrices. Noise in the estimates is hence inevitable.

C. Estimating parameters from flow-loop measurements

The adaptive observer (8), with system vectors and matrices (7) is applied on data from the flow-loop experiments sampled at 10 Hz, during a time interval when a drillstring washout is occurring. The actual washout in the experiment is plotted in Fig. 4, measured as a pressure drop over an opened valve. This information is *not* known to the detection algorithm, but shown for reference. As described in Sec. II, the test setup has $N_a = 4$ pressure measurements in the annulus and $N_d = 1$ pressure measurements in the drillstring. For appropriate scaling in the model, bar is used as unit for pressures, and L/s for flow rates. All parameters in Tab. I are scaled accordingly. The observer is initialized with $\hat{x}(0) = \begin{bmatrix} 16, & 5, & 15 \end{bmatrix}^\top$, $\hat{\theta}(0) = 10^{-4} \times \begin{bmatrix} 9.7, & 23.5, & 1.7, & 0.24, & 0.34, & 4.9 \end{bmatrix}^\top$, and configured with the parameters listed in Tab. I. The observer gains are chosen such that (9) is fulfilled and with sufficiently fast response of the observer such that a stepwise change in a friction parameter could be tracked with a rise time of 1 s. The values used are $K_x = \text{diag}(3,3,3)$, $\Gamma = \Lambda = 5 \times 10^{-5} \times \text{diag}(1,1,10,10,10,10)$, where 'diag' denotes a diagonal matrix.

The estimated topside pump pressures p_p and p_c are shown in the upper panel of Fig. 5, and the flow through the bit in the lower panel. Both pressures are directly measured, giving good estimates as expected. The flow through the bit q_{bit} is not measured. By ignoring flow dynamics in the drillstring, bit flow can be assumed equal to the pump flow, $q_{\text{bit}} = q_p$. This assumption is no longer valid during a washout, resulting in a change in estimated parameters $\hat{\theta}$. The estimated parameters are shown in Fig. 6. These plots show that the effect of a washout is visible in the parameters $\hat{\theta}_d$ and $\hat{\theta}_b$, but much less in $\hat{\theta}_{a,1}, \ldots, \hat{\theta}_{a,4}$. The latter are essential to isolate the washout location.

IV. Statistical change detection

Detecting change of parameters in a linear system is a classical problem in statistics. An overview of methods that are

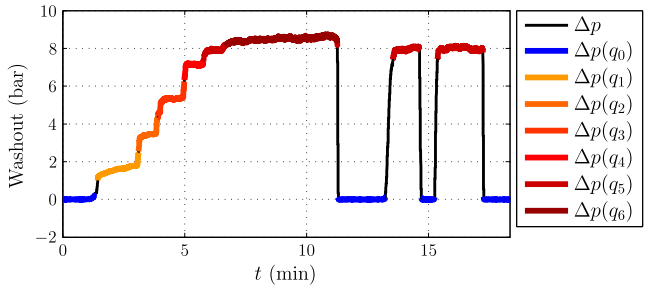

Figure 4. Actual washout in experiment measured over washout emulation valve, measured as pressure loss at different flow rates $\{q_0, \ldots, q_6\}$. The color coding shown to the right shows the pressure drop $\Delta p(q_i)$ for each flow rate q_i, where higher flow rates give higher pressure drop. This information is *not* known to the diagnosis methods, but shown for reference.

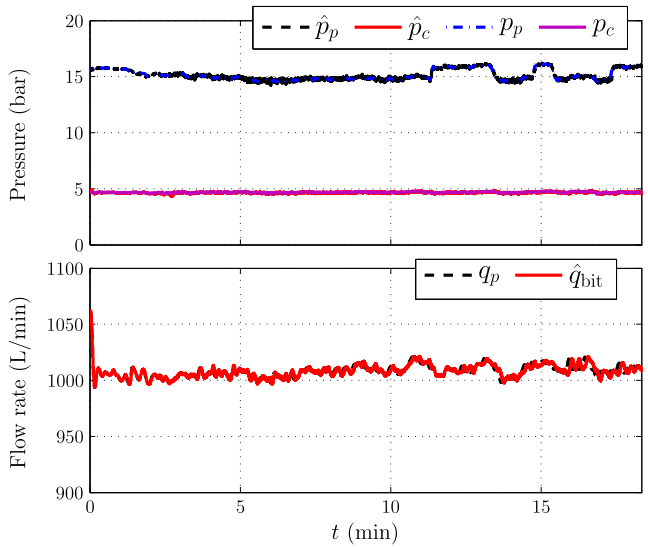

Figure 5. State estimation and measurements of pump pressure (p_p), choke pressure (p_c), and bit flow/pump flow (q_{bit}/q_p) during a washout. The flow rate and choke pressure is constant, while the pump pressure decreases during the washout due to reduced friction in the system.

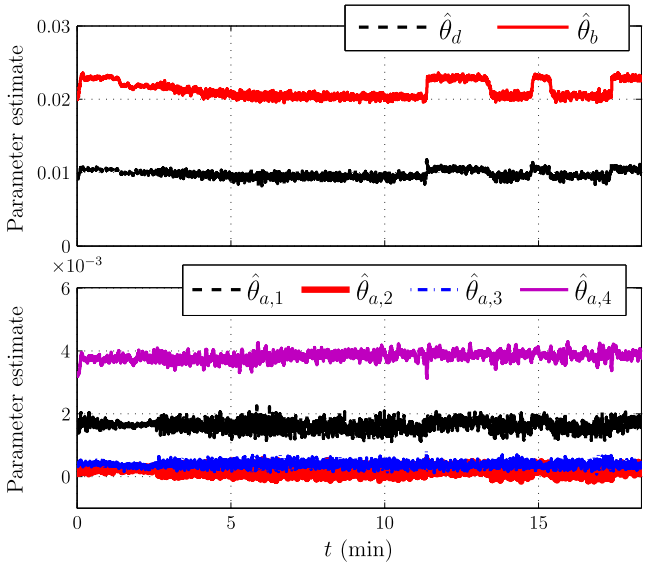

Figure 6. Estimated parameters $\hat{\theta}_d$, $\hat{\theta}_b$ and $\hat{\theta}_{a1}$ to $\hat{\theta}_{a4}$.

applicable for linear systems with Gaussian noise is provided in [27]. When the quantities for which change detection are desired have non-Gaussian distributed noise, the change detection problem is harder but solvable. When the quantities under test are time-wise correlated and non-Gaussian, tests can be achieved but analytical methods may not be available to determine thresholds that give desired false alarm and detection probabilities.

A widely applied methodology is based on a likelihood ratio test, which maximizes the probability of detection P_D with a given false alarm probability P_{FA} [28]. The test will differentiate between the *null hypothesis* $\mathcal{H}_0$ and the *alternative hypothesis* $\mathcal{H}_1$ using the probability density function (PDF) under each hypothesis. If the statistical parameters under $\mathcal{H}_1$ are unknown, the generalized likelihood ratio test (GLRT) can be applied.

The proposed method in this paper is to use parameter estimation to track physical changes in friction. With noise in the measurement, and with desired fast detection, parameter estimates are inevitably subjected to random variation. Thus is statistical change detection used to obtain desired false alarm rate and detection properties. Statistical change detection furthermore gives us isolation capability with known statistical properties. Methods for statistical change detection in fault diagnosis were applied in [29], [30] and applications are referred in [31] where GLRT was employed for detecting change in estimated parameters.

The need for statistical change detection is illustrated by inspecting $\hat{\theta}_d$ and $\hat{\theta}_b$ plotted in Fig. 6, which are affected the most by a drillstring washout. Fig. 7 shows the fault free case $\mathcal{H}_0$, and the fault-case $\mathcal{H}_1(q_i)$ for different washout flow rates q_i, see Fig. 4. The contour lines show two and three standard deviations calculated as if data were Gaussian. The upper plot illustrates that the small washout flow rate q_1 is difficult to detect from the parameters while keeping the false alarm rate low. For the friction parameters $\hat{\theta}_{a,1}$ and $\hat{\theta}_{a,2}$ in the annulus in the lower plot in Fig. 7, it is not possible to distinguish the different cases. Without a statistical change detection approach, it may be possible to detect a washout through change in $\hat{\theta}_d$ and $\hat{\theta}_b$, albeit with poor false alarm versus detection performance, but it would not be possible to determine the washout position.

V. Probability Distribution

The statistical change detection algorithm presented in Sec. VI utilizes the probability density function (PDF) of the noise in order to detect a change. With a vector of estimated parameters $\hat{\theta}$, it is possible to detect a change in each parameter isolated, using *univariate* distributions, or to jointly detect change in the *multivariate* distribution. The different distributions will be presented in this section.

A. Probability distribution of estimated parameters

Most commonly the noise of a signal is assumed to be independent, identically distributed (IID) Gaussian white noise. However, if the noise of the signal has heavier tails it will be more accurately represented with another distribution. The

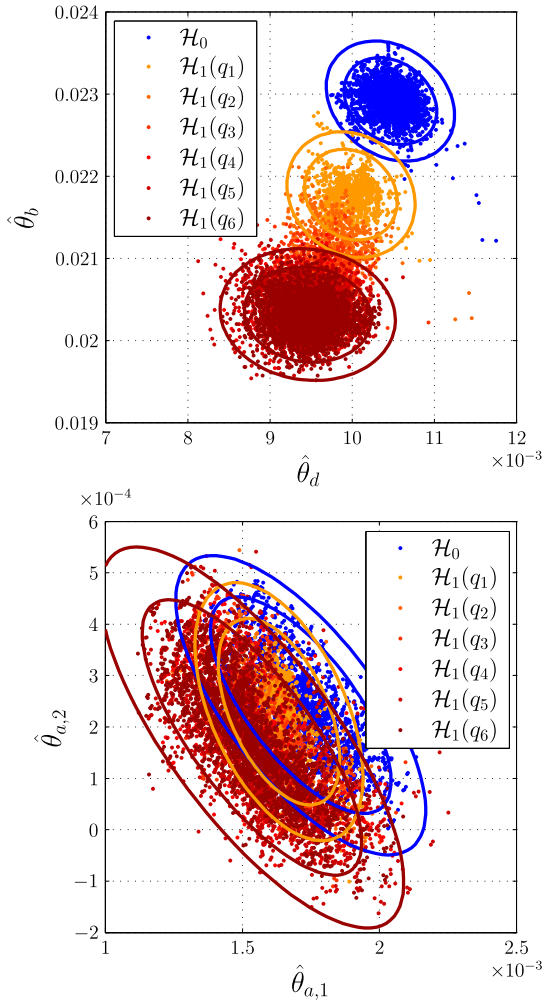

Figure 7. Scatter plot of estimated parameters without washout ($\mathcal{H}_0$), and with different flows of washout ($\mathcal{H}_1(q_i)$), where flow rates are corresponding to the washout pressure drop shown in Fig. 4. Ellipsoids show 2σ and 3σ for no washout (blue), minimum (yellow) and maximum washout (dark red).

estimated parameters are nonlinear functions of the measurements, which are not independent due to the nature of the observer, where the innovations are integrated from one time step to the next. For most distributions, it is rather difficult to find analytical expressions for the *likelihood ratio* $L(x)$ over a window N,

$$L(x) = \frac{f(x_{k-N+1}, \dots x_k; \mathcal{H}_1)}{f(x_{k-N+1}, \dots x_k; \mathcal{H}_0)} = \frac{f(x_k; \mathcal{H}_1 | x_{k-1}, \dots x_{k-N+1}) \cdots f(x_{k-N+1}; \mathcal{H}_1)}{f(x_k; \mathcal{H}_0 | x_{k-1}, \dots x_{k-N+1}) \cdots f(x_{k-N+1}; \mathcal{H}_0)}, \quad (10)$$

if the signal is non-white, since conditional probabilities would have to be included. If the signal has non-white noise, a whitening filter can be applied in order to get close to white noise. IID Gaussian noise for $\hat{\theta}$ was assumed in [16], whereas a closer look on the distribution after white-filtering will be studied in this paper.

To find a candidate distribution, the cumulative distribution of the white-filtered estimated parameter $\hat{\theta}_b$ is plotted as illustration in the probability plot in Fig. 8 for different distributions. The dashed straight line represents the Gaussian

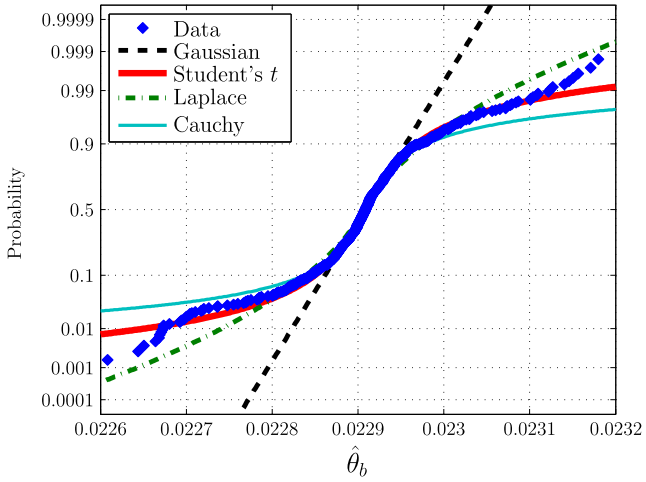

Figure 8. Normal probability plot of white-filtered estimated parameter $\hat{\theta}_b$ for different distributions. Data plotted in blue.

cumulative distribution function (CDF), whereas the heavier-tails distributions Student's t, Laplace and Cauchy will have a curved profile. Laplace and Cauchy distributions have been applied in other detection problems in [30], [32]. Comparing with the estimated parameter in blue, these heavier tail-distributions clearly better fit the data. The Kolmogorov-Smirnov test p-values of the white-filtered estimated parameters for the different distributions are given in Tab. II. Here only Student's t and Cauchy distributions have a p-value above 0.05 for all estimated parameters, which is a typical threshold used to reject the hypothesis that data have the corresponding distribution. Due to the high p-value for the Student's t-distribution, this is chosen as best fit, although the Cauchy distribution could also be a candidate.

Table II
p-VALUE FOR DIFFERENT DISTRIBUTIONS.

Parameter	Gaussian	Student's t	Laplace	Cauchy
$\hat{\theta}_d$	$\sim 10^{-10}$	0.57 ($\nu = 2.2$)	0.14	0.16
$\hat{\theta}_b$	$< 10^{-12}$	0.94 ($\nu = 2.1$)	0.069	0.14
$\hat{\theta}_{a1}$	$< 10^{-12}$	0.26 ($\nu = 1.8$)	0.0024	0.28
$\hat{\theta}_{a2}$	$< 10^{-12}$	0.58 ($\nu = 1.7$)	0.075	0.17
$\hat{\theta}_{a3}$	$\sim 10^{-8}$	0.58 ($\nu = 2.4$)	0.38	0.16
$\hat{\theta}_{a4}$	$< 10^{-12}$	0.44 ($\nu = 1.6$)	0.0031	0.49

B. p-variate t-distribution

Generally, the p-variate t-distribution with center μ, correlation matrix S, and degrees of freedom $\nu > 0$ has the joint probability density function

$$f(x; \mu, S, \nu) = \frac{\Gamma((p+\nu)/2)}{\Gamma(\nu/2)(\pi\nu)^{p/2}|S|^{1/2}} \times \left[1 + \frac{1}{\nu}(x-\mu)^\top S^{-1}(x-\mu)\right]^{-\frac{p+\nu}{2}}, \quad (11)$$

where $\Gamma(z) = \int_0^\infty t^{z-1}e^{-1}dt$ is the Gamma function. For $\nu > 1$, $\mathrm{E}(x) = \mu$, for $\nu > 2, \mathrm{Var}(x) = S\nu/(\nu-2)$ [33].

If each parameter is considered individually, a univariate t-distribution with $p = 1$ can be used to represent the distribution of the estimated parameters. If changes to all parameters are considered simultaneously, the $p = N_\theta$ multivariate distribution will have to be used.

The degrees of freedom ν in the univariate Student's t-distribution are also listed in Tab. II for each estimated parameter. Note that the if $\nu = 1$, (11) is the p-variate Cauchy distribution. If $\nu \to \infty$, (11) is the p-variate Gaussian distribution [33].

VI. Generalized likelihood ratio test

The size of the washout affects the magnitude of change in the friction parameters, but the magnitude of change is unknown. A generalized likelihood ratio test (GLRT) can hence be applied for change detection. The GLRT utilizes the distribution of the noise in the estimated parameters to best fit a t-distribution. In this section, the GLRT for univariate distributions is described, together with multivariate distributions where the direction of change is assumed known or unknown, respectively.

Change detection for parameters with Gaussian noise were thoroughly treated in [27], a GLRT detector was derived for Cauchy distributed test quantities in [34], but a GLRT detector for the t-distribution has not been found in the literature.

A. GLRT with univariate Student's t-distribution

To detect changes in the vector of estimated friction parameters, changes to each parameter can be considered independently, using a generalized likelihood ratio test with univariate Student's t-distributions. The detection problem is to differentiate whether a signal x belongs to the null hypothesis $\mathcal{H}_0$ or the alternative hypothesis $\mathcal{H}_1$. If only the statistical parameter μ changes, whereas σ and ν are assumed constant, the detection problem with $\hat{\theta} \in \mathbb{R}$ is

$$\mathcal{H}_0: \quad \hat{\theta} \sim t(\mu_0, \sigma, \nu), \tag{12a}$$

$$\mathcal{H}_1: \quad \hat{\theta} \sim t(\mu_1, \sigma, \nu). \tag{12b}$$

To reduce computational cost, the window-limited GLRT is used where $0 \leq \tilde{N} < N$ [35], [36], which is given by

$$g(k) = \max_{k-N+1 \leq j \leq k-\tilde{N}} \ln \frac{\prod_{i=j}^{k} f(\hat{\theta}(i); \hat{\mu}_1, \sigma, \nu)}{\prod_{i=j}^{k} f(\hat{\theta}(i); \mu_0, \sigma, \nu)}, \tag{13}$$

where $\hat{\mu}_1$ is the maximum likelihood estimate of the mean μ_1 at $\mathcal{H}_1$, and $f(x; \mu, \sigma, \nu)$ is the univariate PDF (11) with $p = 1$.

A change between the hypotheses (12) is detected if the decision function $g(k)$ is above a threshold h,

$$\begin{aligned} &\text{if} \quad g(k) \leq h \quad \text{accept} \quad \mathcal{H}_0, \\ &\text{if} \quad g(k) > h \quad \text{accept} \quad \mathcal{H}_1. \end{aligned}$$

With univariate distributions, N_θ decision functions $g(k; \theta_i)$ will have to be checked against corresponding thresholds h_i.

B. GLRT with multivariate t-distribution and known direction of change

Detecting a change in a multivariate Gaussian distribution where the direction is known but magnitude unknown, is described in [37], [38]. This is generalized to the multivariate t-distribution in this section, and the derivation is provided in Appendix B.

Let the change detection problem with $\hat{\theta} \in \mathbb{R}^{N_\theta}$ be

$$\begin{aligned} \mathcal{H}_0: \quad & \hat{\theta} \sim t(\mu_0, S, \nu), \\ \mathcal{H}_1: \quad & \hat{\theta} \sim t(\mu_0 + w\Upsilon, S, \nu), \end{aligned}$$

where w is the change magnitude and Υ is the change direction with $\|\Upsilon\| = 1$, assuming that S and ν are unchanged. The generalized likelihood ratio decision function [37], [28] is given by

$$g(k) = \max_{k-N+1 \leq j \leq k-\tilde{N}} \ln \frac{\sup_w \prod_{i=j}^{k} f(\hat{\theta}(i); \mu_0 + w\Upsilon, S, \nu)}{\prod_{i=j}^{k} f(\hat{\theta}(i); \mu_0, S, \nu)}. \tag{14}$$

With a derivation (see Appendix B) similar to that of a multivariate normal distribution in [37], [38], the estimate of magnitude of change with distribution (11) is

$$\hat{w}(k, j) = \frac{\Upsilon^\top S^{-1} (\bar{\Theta}(k, j) - \mu_0)}{\Upsilon^\top S^{-1} \Upsilon}, \tag{15}$$

where

$$\bar{\Theta}(k, j) = \frac{1}{k-j+1} \sum_{i=j}^{k} \hat{\theta}(i). \tag{16}$$

The resulting decision function will then be

$$\begin{aligned} g(k) = \max_{k-N+1 \leq j \leq k-\tilde{N}} & \frac{p+\nu}{2} \sum_{i=j}^{k} \\ & \left[-\ln \left(1 + \frac{1}{\nu} (\hat{\theta}(i) - \mu_0 - \hat{w}\Upsilon)^\top S^{-1} (\hat{\theta}(i) - \mu_0 - \hat{w}\Upsilon) \right) \right. \\ & \left. + \ln \left(1 + \frac{1}{\nu} (\hat{\theta}(i) - \mu_0)^\top S^{-1} (\hat{\theta}(i) - \mu_0 \right)) \right]. \end{aligned} \tag{17}$$

C. GLRT with multivariate t-distribution and unknown direction of change

If no assumption of direction of change is assumed, the MLE $\hat{\mu}_1$ of the mean at $\mathcal{H}_1$ has to be found. From Appendix A, the MLE of the mean μ_1 is given by

$$\hat{\mu}_1 = \frac{1}{k-j+1} \sum_{i=j}^{k} \hat{\theta}(i), \tag{18}$$

and the GLR decision function is given by

$$\begin{aligned} g(k) = \max_{k-N+1 \leq j \leq k-\tilde{N}} & \frac{p+\nu}{2} \sum_{i=j}^{k} \\ & \left[-\ln \left(1 + \frac{1}{\nu} (\hat{\theta}(i) - \hat{\mu}_1)^\top S^{-1} (\hat{\theta}(i) - \hat{\mu}_1) \right) \right. \\ & \left. + \ln \left(1 + \frac{1}{\nu} (\hat{\theta}(i) - \mu_0)^\top S^{-1} (\hat{\theta}(i) - \mu_0) \right) \right]. \end{aligned} \tag{19}$$

D. Thresholds based on GLRT test statistic approximated by a Weibull distribution

If the GLRT input was Gaussian and IID, the test statistic $g(k)$ would asymptotically follow a χ^2_r distribution and with r unknown parameters, r degrees of freedom under $\mathcal{H}_0$, and a non-central $\chi'^2_r(\lambda)$ distribution with non-centrality parameter λ under $\mathcal{H}_1$ [28]. This would make it possible to set a threshold corresponding to a desired probability of false alarms and of detection. However, for real applications with correlated input, $g(k)$ is not χ^2_r distributed. Distributions seen in real applications depend on properties of the case. A Weibull distribution best fitted residuals from aircraft attitude data in [30]; a lognormal distribution best fitted the GLRT test statistic from narrow band correlated ship motion data in [29]. The distribution of the test statistic is therefore studied in this section, based on real data.

Having tested several possibilities, the Weibull distribution was found to give a good fit to the test statistic. The Weibull distribution has the probability distribution $F(x;\alpha,\beta)$ and the density function $f(x;\alpha,\beta)$, given by

$$F(x;\alpha,\beta) = 1 - e^{-(x/\alpha)^\beta}, \quad x \geq 0, \tag{20a}$$

$$f(x;\alpha,\beta) = \frac{\beta}{\alpha}\left(\frac{x}{\alpha}\right)^{\beta-1} e^{-(x/\alpha)^\beta}, \quad x \geq 0, \tag{20b}$$

where $\alpha > 0$ is the scale parameter and $\beta > 0$ the shape parameter.

Let P_{FA} be the probability of false alarm under $\mathcal{H}_0$. Then using the inverse CDF gives a threshold h with the given probability P_{FA},

$$h = Q(1 - P_{FA}; \mathcal{H}_0, \alpha_0, \beta_0) = \beta_0 \left(-\ln(P_{FA})\right)^{1/\alpha_0}. \tag{21}$$

The given threshold h will also determine the probability of detecting a fault under hypothesis $\mathcal{H}_1$ with probability P_D,

$$P_D = 1 - F(h; \mathcal{H}_1, \alpha_1, \beta_1) = e^{-(h/\alpha_1)^{\beta_1}}. \tag{22}$$

VII. Fault diagnosis

Changes to the different parameters are used to detect a washout and isolate its position. As seen in Fig. 2, a washout will decrease the flow in the lower parts of the drillstring and the annulus, as well as in the drill bit. This will result in a decrease in the estimated parameters, since the estimator assumes equal flow throughout the system. Friction changes in the drillstring and bit are considerably higher than in the annulus, and they are thus used for detection. A washout is detected if both $\hat{\theta}_d$ and $\hat{\theta}_b$ have a negative change, as listed in Tab. III. At the position of the washout, the related friction parameter will have a positive change. There will still be some friction loss in this section, however only the pressure sensor in the beginning of the section will be affected by reduced flow. The net effect is an increase in pressure drop in this section, which is used to isolate the washout. The other annular friction parameters must be unchanged or changing in negative direction.

Table III
Fault isolation of drillstring washout with increasing (+), decreasing (−) and unchanged (0) variables. X denotes ignored change in parameter.

	Detection		Isolation			
	$\hat{\theta}_d$	$\hat{\theta}_b$	$\hat{\theta}_{a,1}$	$\hat{\theta}_{a,2}$	$\hat{\theta}_{a,3}$	$\hat{\theta}_{a,4}$
Washout 1 (f_1)	−	−	+	−/0	−/0	−/0
Washout 2 (f_2)	−	−	−/0	+	−/0	−/0
Washout 3 (f_3)	−	−	−/0	−/0	+	−/0
Washout 4 (f_4)	−	−	−/0	−/0	−/0	+
W.o., unknown pos. (f_0)	−	−	X	X	X	X

A. Isolation based on individual parameter changes with univariate distributions

If changes to each parameter are individually considered, a GLRT on each estimated parameter is used for fault diagnosis. There will be one threshold for each estimated parameter, determined based on a specified probability P_{FA} of false alarm. Let the possible faults be

$$f_i \in \mathcal{F}, \tag{23}$$

where f_i represents a washout between sensor $p_{a,i}$ and $p_{a,i+1}$, corresponding to friction parameter $\theta_{a,i}$, and $\mathcal{F}$ are all possible locations of washout. Location of washout position from friction parameters are listed in Tab. III, based on the changes to friction shown in Fig. 2. If the changes in estimated annulus parameters are inconsistent with regards to rows in Tab. III, the position cannot be isolated, although a washout may still detected if $\hat{\theta}_d$ and $\hat{\theta}_b$ have a negative change (f_0).

B. Isolation in multivariate distribution with known direction of change

If the direction of change is limited to the possible known vectors of change directions $\Upsilon_i \in \mathcal{Y}$, isolation is done by finding the Υ_i with the largest change magnitude w. This will reduce the problem of inconsistent changes to parameters as found in the univariate case in Sec. VII-A, due to some parameters being below its threshold.

For each data sample, the largest $\hat{w}(\Upsilon_i)$ is found from (15) with fault isolation position

$$f_{\text{isol}} := \arg\max_i \hat{w}(\Upsilon_i) = \frac{\Upsilon_i^\top S^{-1}(\bar{\Theta}(k,j) - \mu_0)}{\Upsilon_i^\top S^{-1}\Upsilon_i}, \tag{24}$$

and used to find the value of $g(k)$ in (17) with $\hat{w}(\Upsilon_i | i = f_{\text{isol}})$. Hence is it only necessary to calculate $g(k)$ for one type of fault, although (15) will have to be calculated for each Υ_i.

C. Isolation in multivariate distribution with unknown direction of change

In this case, the fault $f_{\text{isol}} \in \mathcal{F}$ can be isolated by finding the largest projection of change in mean $(\hat{\mu}_1 - \mu_0)$ onto the vectors $\Upsilon_i \in \mathcal{Y}$,

$$f_{\text{isol}} = \arg\max_i \frac{\Upsilon_i^\top (\hat{\mu}_1 - \mu_0)}{\Upsilon_i^\top \Upsilon_i}. \tag{25}$$

The difference between this method and the known direction case in Sec. VII-B is that $\hat{\mu}_1$ is used explicitly in the decision

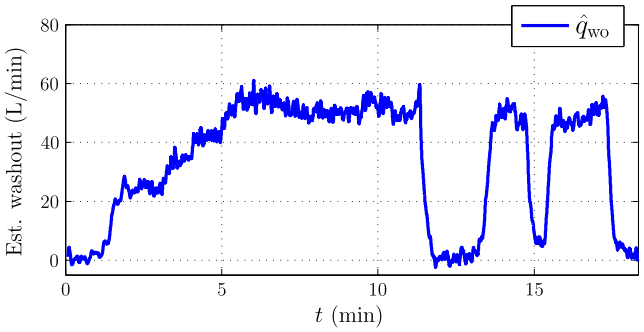

Figure 9. Estimated flow rate of drillstring washout. Can not be validated due to lack of measurements.

function $g(k)$, giving the possibility to detect other faults not specified in $\mathcal{Y}$. If the change direction is close to orthogonal to $\mathcal{Y}$, $g(k)$ in (19) would still be affected, whereas $\hat{w}$ in (15) would be close to zero, giving close to zero value for the decision function (17). However, isolation is still dependent on finding the minimum distance to some possible fault vectors, such as $\mathcal{Y}$. Comparing isolation (24) and (25), the difference is in fact that the changes are scaled with S^{-1} in $\hat{w}$ in (17), taking the correlation into account.

D. Estimating washout magnitude

In addition to isolating the position of the washout, described in Sec. VII, it is also of great value to get an estimate of the leakage magnitude. During normal operation, the flow through the bit will be equal to the pump flow at steady state, $q_{\text{bit}} = q_p$. During a washout, some of the flow is diverted through the leaking hole, giving $q_{\text{wo}} = q_p - q_{\text{bit}}$ at steady state, where q_{wo} denotes the washout flow rate. Since the observer (8) assumes all states measured, including q_{bit}, the estimated friction parameters will change during a washout. Friction loss over the bit will be $\Delta p_{\text{bit}}^{\mathcal{H}_0} = k_{\text{bit}} q_p^2$ with no washout, and $\Delta p_{\text{bit}}^{\mathcal{H}_1} = k_{\text{bit}}(q_p - q_{\text{wo}})^2$ during a washout, where the bit friction parameter k_{bit} is unknown. However, the pressure losses are estimated to be $\Delta \hat{p}_{\text{bit}}^{\mathcal{H}_0} = \hat{\theta}_b^{\mathcal{H}_0} q_p^2$, $\Delta \hat{p}_{\text{bit}}^{\mathcal{H}_1} = \hat{\theta}_b^{\mathcal{H}_1} q_p^2$. An estimate for steady state washout is therefore

$$\hat{q}_{\text{wo}} = q_p \left(1 - \sqrt{\frac{\hat{\theta}_b^{\mathcal{H}_1}}{\hat{\theta}_b^{\mathcal{H}_0}}} \right). \tag{26}$$

The estimated washout (26) is low-pass filtered and plotted in Fig. 9, showing flow rates in the range 0–60 L/min (0–0.001 m^3/s), which is up to 6 % of the total flow. Note that the actual washout plotted in Fig. 4 is measured in pressure loss, not in flow rate, and thus cannot be used to validate (26), although a significant co-variation can be observed. Furthermore is the estimated washout flow rate only valid if a fault is isolated as a washout. If not, the change in estimated parameter $\hat{\theta}_b$ could have other causes.

VIII. Fault Diagnosis Based on Experimental Data

The estimated parameters from the case of drillstring washout are analyzed using the three different methods described in Sec. VI for change detection, namely univariate change detection, multivariate change detection with known direction, and multivariate change detection with unknown change in mean and unknown direction.

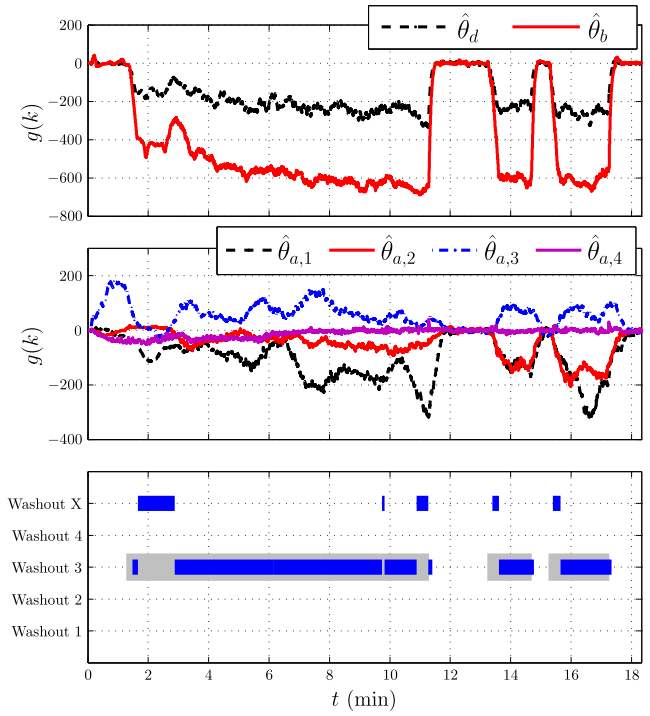

Figure 10. Decision function $g(k)$ for each estimated parameter and resulting fault isolation. Actual washout shown in gray.

A. Change in univariate distributions

The first approach is to consider each parameter individually, testing each estimated parameter against a corresponding threshold. As seen in Tab. III, a washout is detected if $\hat{\theta}_d$ and $\hat{\theta}_b$ have a negative change, and the estimated annular parameters $\hat{\theta}_{a,i}$ are used to locate the washout.

The parameters during $\mathcal{H}_0$ are assumed known in the decision function (13). However, relevant data for the fault free case before the washout is sparse, hence are the statistical parameters μ_0, σ and ν found by using maximum likelihood estimation of the estimated parameters between 685 and 775 seconds (11:30 and 13:00 minutes), and between 1045 and 1100 seconds in a previous test. The GLRT decision function (13) for each estimated parameter is plotted in the two upper panels in Fig. 10, using window lengths $N = 150$ samples for detection and $N = 400$ for isolation, with $\tilde{N} = N/4$. To find thresholds, the probability of false alarm is specified to be $P_{FA} = 10^{-5}$ (0.0024 false alarms per hour) for detection and $P_{FA} = 10^{-3}$ (0.09 false alarms per hour) for isolation. Comparing these plots with the actual washout in Fig. 4, changes to $\hat{\theta}_d$ and $\hat{\theta}_b$ seem quite easy to detect, with large numerical values of $g(k)$ during a washout and small without it. However, $\hat{\theta}_{a,i}$ are less affected making isolation more challenging, although in a real drilling situation the isolation window could easily be chosen 10 to 20 times larger.

In Fig 11, the GLRT of $\hat{\theta}_{a,3}$ with data during $\mathcal{H}_0$ is plotted in a probability plot together with a fitted Weibull distribution.

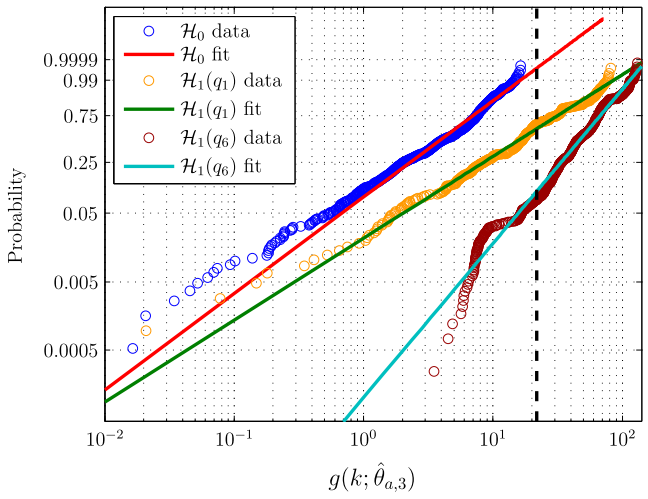

Figure 11. Weibull probability plot of GLRT under $\mathcal{H}_0$, $\mathcal{H}_1(q_1)$ and $\mathcal{H}_1(q_6)$ for estimated parameter $\hat{\theta}_{a,3}$ fitted to Weibull distributions. Threshold shown with dashed line.

This friction parameter will determine isolation of the washout. Also plotted is data under hypothesis $\mathcal{H}_1$ with washout flow rate q_1 corresponding to a pressure loss between 1 and 2 bar, see Fig. 5, and flow rate q_6 with pressure loss of 8 bar. The statistical parameters of the fitted Weibull distributions (20a) during $\mathcal{H}_0$, $\mathcal{H}_1(q_1)$ and $\mathcal{H}_1(q_6)$ are listed in Tab. IV, also showing the corresponding threshold values and detection probabilities P_D. For convenience, the table shows the missed detection probability $P_M = 1 - P_D$.

As illustrated in Fig. 11, $\hat{\theta}_{a,3}$ has a quite small value for probability of detection at q_1, meaning that isolation for small washout flow rates is quite uncertain. If P_D was to increase, the threshold should be lower with a penalty in increased P_{FA}.

Using the thresholds listed in Tab. IV, the resulting fault isolation is shown in the bottom of Fig. 10. Isolation of the position is quite uncertain in the first 3 minutes where the washout is ramping up (q_1 and q_2). When the washout rate reaches a high level, isolation is quite certain. The reason for no isolation for a short period at around 13 and 15 minutes is due to a longer window for isolation than for detection, combined with a sudden change in washout flow rate. The estimated $\hat{\theta}_{a,3}$ is above the threshold for the first two minutes, even though there are no faults. The reason is probably due to external factors (disturbances) in the process.

B. Multivariate distribution with known direction of change

The second case is to use the multivariate distribution, and limit the possible directions of change to a predefined set of vectors $\Upsilon_i \in \mathcal{Y}$, as described in Sec.VI-B, with isolation as described in Sec. VII-B. The assumed possible change directions for detection and isolation are column vectors of

$$\bar{\Upsilon}_{\text{det}} = \begin{bmatrix} -1 \\ -3 \end{bmatrix}, \quad \bar{\Upsilon}_{\text{isol}} = \begin{bmatrix} 1 & -1 & -1 & -1 \\ 0 & 1 & -1 & -1 \\ 0 & 0 & 1 & -1 \\ 0 & 0 & 0 & 1 \end{bmatrix}, \tag{27}$$

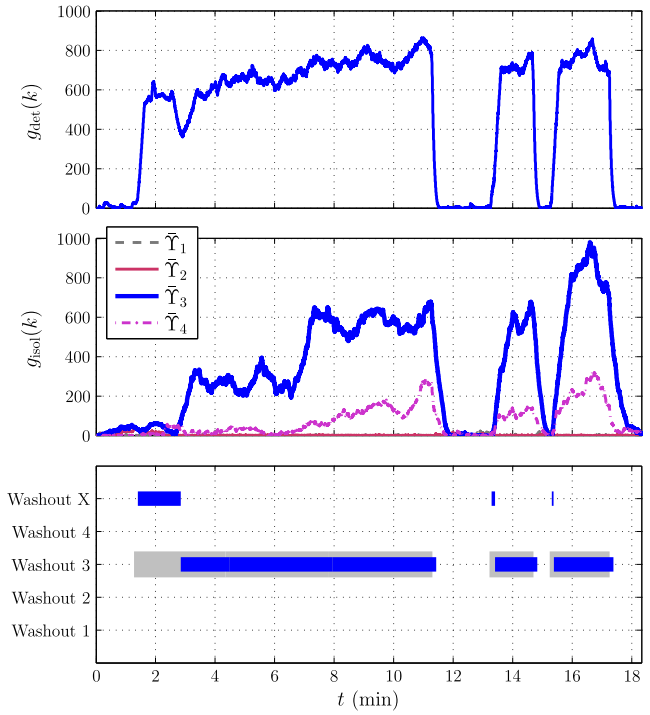

Figure 12. Decision function $g(k)$ with known direction of change Υ. Isolation based on largest $\hat{w}$ for each direction of change $\Upsilon_i \in \mathcal{Y}$, with $g(k)$ plotted for each direction. Actual washout shown in gray.

where $\Upsilon_i = \bar{\Upsilon}_i / ||\bar{\Upsilon}_i||$. The magnitude of the friction parameter in the bit increases approximately three times the magnitude of the friction parameter in the drillstring. It is assumed that all parameters in the annulus are affected equally.

The white-filtered estimated parameters $\hat{\theta}_{\text{det}} \in \mathbb{R}^{N_d+1}$ and $\hat{\theta}_{\text{isol}} \in \mathbb{R}^{N_a}$ are fitted to a multivariate t-distributions using the ECME algorithm [39]. The decision functions for detection and isolation are plotted in Fig. 12, together with resulting isolation. In the middle panel, the isolation functions $g_{\text{isol}}(k)$ are plotted for each $\Upsilon_i \in \mathcal{Y}$, showing that a washout at position three gives the highest value. Note that isolation is based on maximum $\hat{w}(\Upsilon_i)$ given by (24), and thus only one decision function is required to be calculated. Parameter values, thresholds and detection probabilities are listed in Tab. V. The threshold value h for $g_{\text{det}}(k)$ was selected to give a false alarm probability $P_{FA} = 10^{-5}$ from the data under $\mathcal{H}_0$, for isolation $P_{\text{FA}} = 10^{-3}$ is used.

No washout is isolated in the first three minutes. The reason may be that changes in the parameters do not correspond directly to the directions (27). Furthermore may these directions not be entirely accurate, where also correlation S affects the change direction (15). Compared to the univariate case in Fig. 10, accuracy in isolated position is increased for higher washout flow rates (after six minutes). The detection probability P_D is higher for the multivariate method, and for higher washout rates the detection probability in isolation is significantly higher (lower P_M).

Table IV
THRESHOLD AND PROBABILITY OF DETECTION BASED ON FITTED WEIBULL DISTRIBUTIONS WITH PARAMETERS α AND β, WITH CHANGES TO INDEPENDENT UNIVARIATE DISTRIBUTIONS.

	P_{FA}	N	h	α_0	β_0	$\alpha_1(q_1)$	$\beta_1(q_1)$	$\alpha_1(q_6)$	$\beta_1(q_6)$	$P_M(q_1)$	$P_M(q_6)$
$\hat{\theta}_d$	10^{-5}	150	39.0	3.68	1.04	141	4.65	264	8.62	2.54×10^{-3}	$\sim 10^{-9}$
$\hat{\theta}_b$	10^{-5}	150	38.3	3.1	0.971	405	8.07	645	28	$\sim 10^{-10}$	$< 10^{-12}$
$\hat{\theta}_{a,1}$	10^{-3}	400	40.1	6.49	1.06	78.7	4.36	187	4.21	0.0515	1.54×10^{-3}
$\hat{\theta}_{a,2}$	10^{-3}	400	15.7	3.98	1.41	11.5	1.28	65.2	5.56	0.775	3.66×10^{-4}
$\hat{\theta}_{a,3}$	10^{-3}	400	21.8	5.56	1.41	24	1.2	58.3	2.26	0.59	0.102
$\hat{\theta}_{a,4}$	10^{-3}	400	11.0	4.19	2.0	31.9	3.52	4.99	1.61	0.0233	0.972

Table V
THRESHOLD AND PROBABILITY OF MISSED DETECTION P_M BASED ON WEIBULL FIT WITH KNOWN CHANGE DIRECTION Υ OF A MULTIVARIATE DISTRIBUTION.

	P_{FA}	N	h	α_0	β_0	$\alpha_1(q_1)$	$\beta_1(q_1)$	$\alpha_1(q_6)$	$\beta_1(q_6)$	$P_M(q_1)$	$P_M(q_6)$
Detection	10^{-5}	150	65.6	3.81	0.858	527	7.70	782	17.6	$\sim 10^{-7}$	$< 10^{-12}$
Isolation	10^{-3}	400	76.5	14.1	1.14	55.8	1.14	592	14.2	0.761	$\sim 10^{-12}$

C. Multivariate distribution with unknown change in mean and unknown direction

In the third case, no assumption about change direction is made in the decision function, making it sensitive to all changes. Isolation given by (25) is done by finding the change in mean closest to possible change vectors, here given by (27).

The decision function $g_{\text{det}}(k)$ for the multivariate distribution of $\hat{\theta}_d$ and $\hat{\theta}_b$ is plotted in the top of Fig. 13, which is used for detection. Parameters $\hat{\theta}_{a,i}$ are used for isolation, with detection function $g_{\text{isol}}(k)$ plotted in the middle panel. Isolation is plotted in the lower panel. The thresholds are based on fitted data to Weibull probability functions, plotted for $g_{\text{isol}}(k)$ in Fig. 14. Comparing with the univariate method in Fig. 11, much less of the $\mathcal{H}_1$ data is left of the threshold, giving better isolation. Parameter values, thresholds and detection probabilities are listed in Tab. VI.

With this method a washout is detected almost immediately and is isolated around the 3 minutes time stamp. The difference between this very successful approach and the previous method is that assumption about direction is only made for isolation. Furthermore, isolation is only done based on changes in mean (25), not scaled with S as in (24).

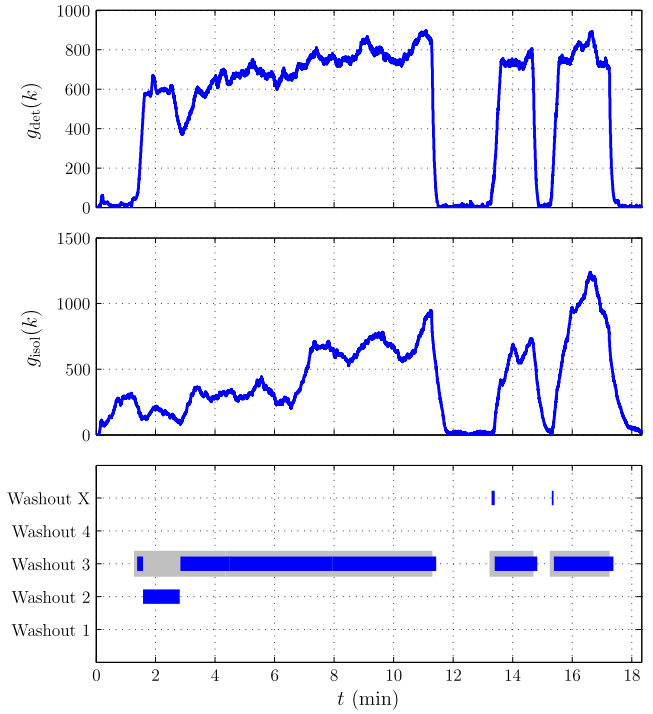

Figure 13. Decision function $g(k)$ with unknown change in mean and unknown direction of change. Isolation based on finding change in mean closest to possible change directions $\Upsilon_i \in \mathcal{Y}$. Actual washout shown in gray.

IX. DISCUSSION

The friction model used in the adaptive observer is quite simple, but proved to work satisfactory for the washout case. If the method was to be applied during a large range of pump flow rates and with different drilling fluid densities, a more sophisticated friction model may be required. Nevertheless, for the current process, it has been sufficient in order to provide convincing detection of washout and isolation of the position of the leakage.

Two vector-based (multivariate) methods were compared. Method one, $GLRT_{w\Upsilon}$, assumed a known direction Υ, but unknown magnitude w. The direction vectors were determined from expected changes to the parameters with different washout locations. The second method, $GLRT_{\mu_1}$, assumed an unknown direction and magnitude of change in the vector μ_1.

The main difference between the two multivariate methods was that method one limits detection to already specified fault directions, other faults may not be detected. Method two calculates $g(k)$ based on the new estimated direction of change, and then isolates the position based on already assumed known directions. A disturbance not corresponding to the defined directions would impact the decision function in the second case, but much less in the first. A challenge can be to find the correct change directions. In this study, there was only data from one washout location available, the others are assumed with same structure and values.

Detection was based on both drillstring and bit parameters

Table VI
THRESHOLD AND PROBABILITY OF MISSED DETECTION P_M BASED ON WEIBULL FIT WITH CHANGE IN μ_1 OF A MULTIVARIATE DISTRIBUTION.

	P_{FA}	N	h	α_0	β_0	$\alpha_1(q_1)$	$\beta_1(q_1)$	$\alpha_1(q_6)$	$\beta_1(q_6)$	$P_M(q_1)$	$P_M(q_6)$
Detection	10^{-5}	150	61.6	6.64	1.10	550	7.11	810	16.5	$\sim 10^{-7}$	$< 10^{-12}$
Isolation	10^{-3}	400	88.5	24.2	1.49	154	5.82	711	7.34	0.0392	$\sim 10^{-7}$

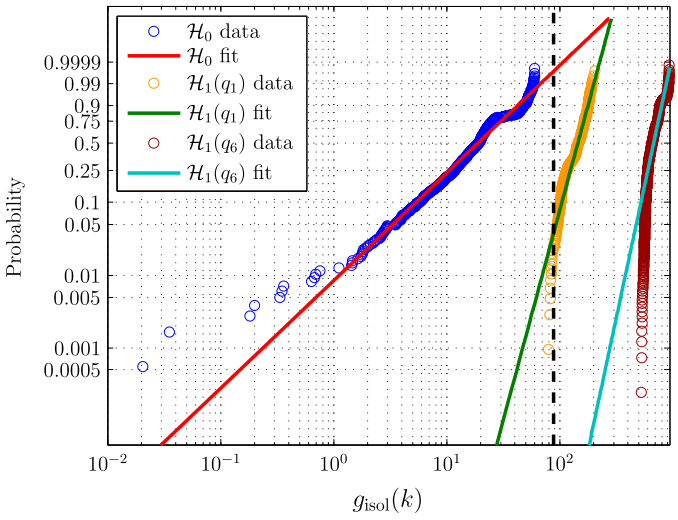

Figure 14. GLRT for isolation under $\mathcal{H}_0$, $\mathcal{H}_1(q_1)$ and $\mathcal{H}_1(q_6)$ for multivariate distribution with unknown direction of change, fitted to Weibull distributions in a Weibull probability plot. Threshold shown with dashed line.

changing in the negative direction, and probability of detection was clearly best using the multivariate methods.

Isolation was also efficiently done with the multivariate methods, with the multivariate $GLRT_{\mu_1}$ approach being clearly superior in isolation performance. Isolation during the first three minutes was difficult, both due to transients in the system during the test but definitely also due to the tiny changes in friction compared to a significant noise level in the parameter estimates. In a real drilling operation, the window size could be 10 minutes or more instead of the 40 seconds used here for reasons of the short duration of each washout level during the experiments. The longer isolation window would give significantly better isolation properties while fast detection could still be obtained since different window sizes are used for detection and isolation.

Based on the experiments reported here, it would be feasible to implement a diagnostic method using $\mathcal{H}_0$ data from normal operation to learn a feasible threshold h from test statistic data for given operational conditions. The detection scheme would be sufficiently sensitive to detect and locate a drillstring washout.

The methods presented in this paper have been successfully tested on the difficult drillstring washout case, but are applicable on all downhole incidents during drilling, that would cause detectable changes to friction and flow. This is studied in [17], detecting and isolating numerous incidents. It is noted that the validation of the proposed method is based on drilling conditions and problems represented by the test rig. In other drilling configurations, the models used for parameter estimation and incident isolation may need to be adjusted. Examples include drilling operation that uses a hole-opener or an under-reamer inside the bottom hole assembly. Such tools have side ports and this would need to be accounted for in the model. The state of cutter arms (extended or retracted) might also need be included in the model and, if a downhole motor is used, the associated bottom leakage at the motor shaft should be included.

X. CONCLUSION

This paper has developed change detection methods for washout detection and localization in oil and gas drilling, and tested the methods on data from a managed pressure drilling test facility. Using estimated friction coefficients in pipe segments as indicators for change, the combination of an adaptive observer to estimate friction parameters and stochastic change detection provides a setup that is able to detect and locate a washout with convincing performance. The parameters were determined to be t-distributed, and generalized likelihood ratio tests were derived for this particular distribution. Different diagnostic algorithms were tested, showing that a multivariate test with unknown change direction and unknown magnitude gave the most accurate detection and isolation as judged from experimental data. The methods presented in this paper are believed to be generic but application to other drilling conditions and problems would require that the model used for parameter estimation and the incident isolation approach are adopted to the specific conditions of the operation.

APPENDIX

A. GLRT for unknown change in mean of a multivariate t-distribution

Given a sequence of N IID observations of a vector $z(j)$, $j = k-N+1, ..., k$. Determine whether z most likely belongs to $p(z;\mathcal{H}_0)$ or to $p(z;\mathcal{H}_1)$, where

$$\mathcal{H}_0: \quad p(z(j)) \sim t(\mu_0, S, \nu), \quad j = k-N+1, ..., k, \tag{28}$$
$$\mathcal{H}_1: \quad p(z(j)) \sim t(\mu_1, S, \nu), \quad j = k-N+1, ..., k, \tag{29}$$

where μ_0 is a known vector, μ_1 is unknown, S and ν are known parameters of the multivariate t-distribution (11). The generalized likelihood ratio decision function [37] is given by

$$\begin{aligned} g(k) &= \max_{k-N+1\le j\le k} \ln \frac{\sup_{\mu_1} \prod_{i=j}^{k} f(z(i);\mu_1,S,\nu)}{\prod_{i=j}^{k} f(z(i);\mu_0,S,\nu)} \\ &= \max_{k-N+1\le j\le k} \sup_{\mu_1} G_j^k(\mu_1), \end{aligned} \tag{30}$$

detecting a change in mean vector μ from μ_0 to μ_1, with S and ν constant. Using that

$$\frac{f(z(i);\mu_1,S,\nu)}{f(z(i);\mu_0,S,\nu)} = \frac{\left[1+\frac{1}{\nu}(z(i)-\mu_1)^\top S^{-1}(z(i)-\mu_1)\right]^{-\frac{p+\nu}{2}}}{\left[1+\frac{1}{\nu}(z(i)-\mu_0)^\top S^{-1}(z(i)-\mu_0)\right]^{-\frac{p+\nu}{2}}}$$

for the multivariate t-distribution with S and ν constant, $G_j^k(\mu_1)$ is given by

$$\begin{aligned} G_j^k(\mu_1) &= \sum_{i=j}^{k} \ln \frac{f(z(i);\mu_1,S,\nu)}{f(z(i);\mu_0,S,\nu)} \\ &= \frac{p+\nu}{2} \sum_{i=j}^{k} \left[-\ln\left(1+\frac{1}{\nu}(z(i)-\mu_1)^\top S^{-1}(z(i)-\mu_1)\right) \right. \\ &\left. + \ln\left(1+\frac{1}{\nu}(z(i)-\mu_0)^\top S^{-1}(z(i)-\mu_0)\right)\right]. \end{aligned}$$

The supremum is found by equating $\frac{\partial G_j^k(\mu_1)}{\partial \mu_1}$ to zero, yielding

$$\begin{aligned} &\sum_{i=j}^{k} \frac{\partial}{\partial \mu_1} \ln\left(1+\frac{1}{\nu}(z(i)-\mu_1)^\top S^{-1}(z(i)-\mu_1)\right) = 0 \\ &\qquad \Longrightarrow \sum_{i=j}^{k} \frac{-2S^{-1}(z(i)-\mu_1)}{\nu+(z(i)-\mu_1)^\top S^{-1}(z(i)-\mu_1)} = 0. \end{aligned}$$

Hence is the maximum likelihood estimate (MLE) of the mean μ_1 given by

$$\hat{\mu}_1 = \frac{1}{k-j+1} \sum_{i=j}^{k} z(i), \tag{31}$$

and the GLRT decision function

$$\begin{aligned} g(k) = \max_{k-N+1\le j\le k} & \frac{p+\nu}{2} \sum_{i=j}^{k} \\ & \left[-\ln\left(1+\frac{1}{\nu}(z(i)-\hat{\mu}_1)^\top S^{-1}(z(i)-\hat{\mu}_1)\right) \right. \\ & \left. + \ln\left(1+\frac{1}{\nu}(z(i)-\mu_0)^\top S^{-1}(z(i)-\mu_0)\right)\right]. \end{aligned} \tag{32}$$

B. Change in mean with known direction but unknown magnitude

If the direction of change is known, the mean after change is represented by $\mu_1 = \mu_0 + w\Upsilon$, where Υ is the unit direction vector and w is the unknown magnitude. Now the GLRT decision function will be slightly different, using that

$$\begin{aligned} &\frac{\partial}{\partial w}(z(i)-\mu_0-w\Upsilon)^\top S^{-1}(z(i)-\mu_0-w\Upsilon) \\ &\qquad = 2w\Upsilon^\top S^{-1}\Upsilon - 2\Upsilon^\top S^{-1}(z(i)-\mu_0) \end{aligned} \tag{33}$$

$$\begin{aligned} &\frac{\partial G_j^k(w)}{\partial w} = 0 \\ &\Longrightarrow \sum_{i=j}^{k} \left[w\Upsilon^\top S^{-1}\Upsilon - \Upsilon^\top S^{-1}(z(i)-\mu_0)\right] = 0. \end{aligned} \tag{34}$$

The MLE of change magnitude is given by

$$\hat{w}(k,j) = \frac{\Upsilon^\top S^{-1}(\bar{Z}_j^k - \mu_0)}{\Upsilon^\top S^{-1}\Upsilon}, \tag{35}$$

$$\bar{Z}_j^k = \frac{1}{k-j+1} \sum_{i=j}^{k} z(i). \tag{36}$$

Using (32) with $\hat{\mu}_1 = \mu_0 + \hat{w}\Upsilon$, and $\hat{w}$ from (35), the GLRT test statistic will hence be

$$\begin{aligned} g(k) = \max_{k-N+1\le j\le k} & \frac{p+\nu}{2} \sum_{i=j}^{k} \\ & \left[-\ln\left(1+\frac{1}{\nu}(z(i)-\mu_0-\hat{w}\Upsilon)^\top S^{-1}(z(i)-\mu_0-\hat{w}\Upsilon)\right) \right. \\ & \left. + \ln\left(1+\frac{1}{\nu}(z(i)-\mu_0)^\top S^{-1}(z(i)-\mu_0)\right)\right]. \end{aligned} \tag{37}$$

REFERENCES

[1] J.-M. Godhavn, "Control Requirements for Automatic Managed Pressure Drilling System," *SPE Drilling and Completion*, vol. 25, no. 3, pp. 336–345, Sep. 2010.

[2] J.-M. Godhavn, A. Pavlov, G.-O. Kaasa, and N. L. Rolland, "Drilling Seeking Automatic Control Solutions," in *Proc. IFAC World Congress*, Milan, Italy, 2011, pp. 10 842–10 850.

[3] D. Bert, A. Storaune, and N. Zheng, "Case Study: Drillstring Failure Analysis and New Deep-Well Guidelines Lead to Success," *SPE Drilling and Completion*, vol. 24, no. 4, Dec. 2009.

[4] K. Macdonald and J. Bjune, "Failure analysis of drillstrings," *Eng. Failure Analysis*, vol. 14, no. 8, pp. 1641–1666, 2007.

[5] D. Hargreaves, S. Jardine, and B. Jeffryes, "Early Kick Detection for Deepwater Drilling: New Probabilistic Methods Applied in the Field," in *Proc. SPE Annu. Tech. Conf. and Exhib., SPE 71369*, New Orleans, LA, 2001.

[6] J. Gravdal, M. Nikolaou, Ø. Breyholtz, and L. Carlsen, "Improved Kick Management During MPD by Real-Time Pore-Pressure Estimation," *SPE Drilling and Completion*, vol. 25, no. 4, pp. 4–7, Dec. 2010.

[7] E. Cayeux, E. W. Dvergsnes, and G. Sælevik, "Early Symptom Detection on the Basis of Real-Time Evaluation of Downhole Conditions : Principles and Results From Several North Sea Drilling Operations," *SPE Drilling and Completion*, vol. 27, no. 4, pp. 546–558, 2012.

[8] E. Hauge, O. M. Aamo, J.-M. Godhavn, and G. Nygaard, "A novel model-based scheme for kick and loss mitigation during drilling," *J. Process Control*, vol. 23, no. 4, pp. 463–472, Apr. 2013.

[9] E. Cayeux, B. Daireaux, E. Dvergsnes, A. Leulseged, B. Bruun, and M. Herbert, "Advanced Drilling Simulation Environment for Testing New Drilling Automation Techniques and Practices," *SPE Drilling and Completion*, vol. 27, no. 4, pp. 6–8, 2012.

[10] P. Skalle, A. Aamodt, and O. E. Gundersen, "Detection of Symptoms for Revealing Causes Leading to Drilling Failures," *SPE Drilling and Completion*, vol. 28, no. 2, pp. 182–193, 2013.

[11] A. Ambrus, P. Ashok, and E. van Oort, "Drilling Rig Sensor Data Validation in the Presence of Real-Time Process Variations," in *Proc. SPE Annu. Tech. Conf. and Exhib., SPE 166387*, New Orleans, LA, 2013.

[12] C. Dalton, M. Paulk, and G. Stevenson, "The Benefits of Real-Time Downhole Pressure and Tension Data With Wired Composite Tubing," *J. Canadian Petroleum Technology*, vol. 42, no. 5, May 2003.

[13] D. Veeningen, J. Palmer, G. Steinicke, J. Saenz, and T. Hansen, "From Field Test to Successful Integration of Broadband Drillstring System for Offshore Extended Reach Wells," in *Proc. SPE Annu. Tech. Conf. and Exhib., SPE 151386*, San Diego, CA, 2012.

[14] T. O. Gulsrud, R. Nybø, and K. S. Bjørkevoll, "Statistical Method for Detection of Poor Hole Cleaning and Stuck Pipe," in *Proc. of Offshore Europe, SPE 123374*, Aberdeen, UK, 2009.

[15] A. Willersrud and L. Imsland, "Fault Diagnosis in Managed Pressure Drilling Using Nonlinear Adaptive Observers," in *Proc. European Control Conference*, Zürich, Switzerland, 2013, pp. 1946–1951.

[16] A. Willersrud, L. Imsland, A. Pavlov, and G.-O. Kaasa, "A Framework for Fault Diagnosis in Managed Pressure Drilling Applied to Flow-Loop Data," in *Dynamics and Control of Process Systems (DYCOPS)*, Mumbai, India, 2013, pp. 625–630.

[17] A. Willersrud, M. Blanke, L. Imsland, and A. Pavlov, "Fault diagnosis of downhole drilling incidents using adaptive observers and statistical change detection," *J. Process Control (in press)*, 2015.

[18] G.-O. Kaasa, Ø. N. Stamnes, O. M. Aamo, and L. Imsland, "Simplified Hydraulics Model Used for Intelligent Estimation of Downhole Pressure for a Managed-Pressure-Drilling Control System," *SPE Drilling and Completion*, vol. 27, no. 1, pp. 127–138, Mar. 2012.

[19] H. F. Grip, T. A. Johansen, L. Imsland, and G.-O. Kaasa, "Parameter estimation and compensation in systems with nonlinearly parameterized perturbations," *Automatica*, vol. 46, no. 1, pp. 19–28, Jan. 2010.

[20] J. Zhou, Ø. N. Stamnes, O. M. Aamo, and G.-O. Kaasa, "Switched Control for Pressure Regulation and Kick Attenuation in a Managed Pressure Drilling System," *IEEE Trans. Control Syst. Technol*, vol. 19, no. 2, pp. 337–350, Mar. 2011.

[21] Ø. N. Stamnes, O. M. Aamo, and G.-O. Kaasa, "Adaptive Redesign of Nonlinear Observers," *IEEE Trans. Autom. Control*, vol. 56, no. 5, pp. 1152–1157, May 2011.

[22] A. T. Bourgoyne Jr., M. E. Chenevert, K. K. Millheim, and F. Young, *Applied Drilling Engineering*, 2nd ed. SPE, 1986.

[23] L. Ljung, "Asymptotic behavior of the extended Kalman filter as a parameter estimator for linear systems," *IEEE Trans. Autom. Control*, vol. 24, no. 1, pp. 36–50, Feb. 1979.

[24] W.-W. Zhou and M. Blanke, "Identification of a class of nonlinear state-space models using RPE techniques," *IEEE Trans. Autom. Control*, vol. 34, no. 3, pp. 312–316, Mar. 1989.

[25] G. Besançon, "Remarks on nonlinear adaptive observer design," *Syst. Control Lett.*, vol. 41, no. 4, pp. 271–280, 2000.

[26] R. Rajamani and J. Hedrick, "Adaptive observers for active automotive suspensions: theory and experiment," *IEEE Trans. Control Syst. Technol.*, vol. 3, no. 1, pp. 86–93, Mar. 1995.

[27] M. Basseville and I. Nikiforov, "Fault isolation for diagnosis: Nuisance rejection and multiple hypotheses testing," *Annu. Reviews Control*, vol. 26, no. 2, pp. 189–202, 2002.

[28] S. M. Kay, *Fundamentals of Statistical Signal Processing: Detection Theory*. Upper Saddle River, NJ: Prentice Hall, 1998.

[29] R. Galeazzi, M. Blanke, and N. K. Poulsen, "Early Detection of Parametric Roll Resonance on Container Ships," *IEEE Trans. Control Syst. Technol.*, vol. 21, no. 2, pp. 489–503, Mar. 2013.

[30] S. Hansen and M. Blanke, "Diagnosis of Airspeed Measurement Faults for Unmanned Aerial Vehicles," *IEEE Trans. Aerosp. Electron. Syst.*, vol. 50, no. 1, 2014.

[31] I. Hwang, S. Kim, Y. Kim, and C. E. Seah, "A Survey of Fault Detection, Isolation, and Reconfiguration Methods," *IEEE Trans. Control Syst. Technol.*, vol. 18, no. 3, pp. 636–653, May 2010.

[32] S. Hansen and M. Blanke, "In-Flight Fault Diagnosis for Autonomous Aircraft Via Low-Rate Telemetry Channel," in *Proc. IFAC SAFEPROCESS*, Mexico City, Mexico, 2012, pp. 576–581.

[33] S. Kotz and S. Nadarajah, *Multivariate t-distribution and their applications*. Cambridge, United Kingdom: Cambridge University Press, 2004.

[34] M. Blanke and S. Hansen, "Towards self-tuning residual generators for UAV control surface fault diagnosis," in *Proc. Conf. Control Fault-Tolerant Systems*, Nice, France, 2013, pp. 37–42.

[35] A. Willsky and H. Jones, "A generalized likelihood ratio approach to the detection and estimation of jumps in linear systems," *IEEE Trans. Autom. Control*, vol. 21, no. 1, pp. 108–112, Feb. 1976.

[36] T. L. Lai, "Sequential Changepoint Detection in Quality Control and Dynamical Systems," *J. Roy. Statistical Soc.*, vol. 57, no. 4, pp. 613–658, 1995.

[37] M. Basseville and I. V. Nikiforov, *Detection of Abrupt Changes: Theory and Applications*. Englewood Cliffs, NJ: Prentice Hall, 1993.

[38] M. Blanke, M. Kinnaert, J. Lunze, and M. Staroswiecki, *Diagnosis and fault-tolerant control*, 2nd ed. Berlin: Springer, 2006.

[39] C. Liu and D. B. Rubin, "ML estimation of the t distribution using EM and its extensions, ECM and ECME," *Statistica Sinica*, vol. 5, pp. 19–39, 1995.

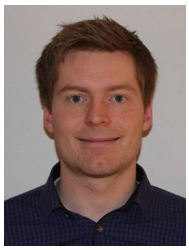

Anders Willersrud received the MSc degree in 2010 from the Department on Engineering Cybernetics at the Norwegian University of Science and Technology (NTNU). He was a trainee in ABB Oil and Gas in 2010-2011. Willersrud is currently a PhD candidate at the Department on Engineering Cybernetics at NTNU, working with fault diagnosis methods in oil and gas drilling.

Mogens Blanke (M 1974, SM 1985) received the MScEE degree in 1974 and the PhD degree in 1982 from the Technical University of Denmark, DTU. He was Systems Analyst with the European Space Agency 1975–76, with DTU 1977-84, was Head of Division at Lyngsø Marine 1985-89, Professor at Aalborg University 1990–99. Since 2000, he has been Professor in Automation and Control at DTU and since 2005 also Adjunct Professor at the Norwegian University of Science and Technology. His research has diagnosis and fault tolerant control as areas of special focus.
Prof. Blanke has held various positions in the International Federation of Automatic Control, including Chair of the TC on Marine Systems, CC Chair and Member of Council. He is a member of the IFAC SAFEPROCESS and Marine Systems TCs. He is Technical Editor for IEEE Transactions of Aerospace and Electronic Systems and Associate Editor for Control Engineering Practice.

Lars Imsland holds a PhD degree in electrical engineering from the Department of Engineering Cybernetics at the Norwegian University of Science and Technology (NTNU). For parts of his PhD studies, he was a vising research scholar at the Institute for Systems Theory in Engineering at the University of Stuttgart, Germany. After earning his PhD, Imsland worked as a post-doctoral researcher at NTNU, as a research scientist at SINTEF and as a specialist for Cybernetica AS, before becoming a full-time professor in control engineering at NTNU in 2009. His main research interests are theory and application of nonlinear and optimizing control and estimation. Examples of applications are within the oil and gas industry (both drilling and production), active safety in the automotive industry, and the use of mobile sensor networks for monitoring of local ice features.

Alexey Pavlov received the MSc degree (cum laude) in applied mathematics from St. Petersburg State University, Russia, in 1998, and the PhD degree in mechanical engineering from the Eindhoven University of Technology, The Netherlands, in 2004. He was a Researcher with the Russian Academy of Sciences, St. Petersburg, Russia, in 1999, the Ford Research Laboratory, Dearborn, USA, in 2000, the Eindhoven University of Technology in 2005, and the Norwegian University of Science and Technology, from 2005 to 2009. Since 2009, he has been a Principal Researcher with the Statoil Research Center, Norway. He has authored or co-authored more than 80 refereed papers and patents, and a book Uniform Output Regulation of Nonlinear Systems: a Convergent Dynamics Approach co-authored with N. van de Wouw and H. Nijmeijer (Birkhauser, 2005). His current research interests include applied nonlinear control and automation of oil and gas production and drilling.